water

MDPI

Article

Groundwater Overexploitation and Seawater Intrusion in Coastal Areas of Arid and Semi-Arid Regions

Nawal Alfarrah [1,2,*] and Kristine Walraevens [1]

[1] Laboratory for Applied Geology and Hydrogeology, Department of Geology, Ghent University, Krijgslaan 281 S8, 9000 Ghent, Belgium; kristine.walraevens@ugent.be
[2] Geology Department, Az Zawiyah University, Az Zawiyah, Libya
* Correspondence: nawalr2003@yahoo.com

Received: 19 December 2017; Accepted: 25 January 2018; Published: 2 February 2018

Abstract: The exploitation of groundwater resources is of high importance and has become very crucial in the last decades, especially in coastal areas of arid and semi-arid regions. The coastal aquifers in these regions are particularly at risk due to intrusion of salty marine water. One example is the case of Tripoli city at the Mediterranean coast of Jifarah Plain, North West Libya. Libya has experienced progressive seawater intrusion in the coastal aquifers since the 1930s because of its ever increasing water demand from underground water resources. Tripoli city is a typical area where the contamination of the aquifer in the form of saltwater intrusion is very developed. Sixty-four groundwater samples were collected from the study area and analyzed for certain parameters that indicate salinization and pollution of the aquifer. The results demonstrate high values of the parameters Electrical Conductivity, Na^+, K^+, Mg^{2+}, Cl^- and $SO_4{}^{2-}$, which can be attributed to seawater intrusion, where Cl^- is the major pollutant of the aquifer. The water types according to the Stuyfzand groundwater classification are mostly CaCl, NaCl and Ca/MgMix. These water types indicate that groundwater chemistry is changed by cation exchange reactions during the mixing process between freshwater and seawater. The intensive extraction of groundwater from the aquifer reduces freshwater outflow to the sea, creates drawdown cones and lowering of the water table to as much as 25 m below mean sea level. Irrigation with nitrogen fertilizers and domestic sewage and movement of contaminants in areas of high hydraulic gradients within the drawdown cones probably are responsible for the high $NO_3{}^-$ concentration in the region.

Keywords: seawater intrusion; coastal aquifer; arid and semi-arid regions; cation exchange; Tripoli; Libya

1. Overview Saltwater Intrusion into Coastal Aquifers

Coastal aquifers serve as major sources for freshwater supply in many countries around the world, especially in the Mediterranean [1]. The fact that coastal zones contain some of the most densely populated areas in the world makes the need for freshwater even more acute [1]. The intensive extraction of groundwater from coastal aquifers reduces freshwater outflow to the sea and creates local water table depression, causing seawater to migrate inland and rising toward the wells [2–4], resulting in deterioration in groundwater quality. This phenomenon, called seawater intrusion, has become one of the major constraints imposed on groundwater utilization in coastal areas.

Saltwater intrusion is one of the most widespread and important processes that degrade water quality to levels exceeding acceptable drinking and irrigation water standards, and endanger future water exploitation in coastal aquifers. Coupled with a continuing sea level rise due to global warming, coastal aquifers are even more under threat. This problem is intensified due to population growth, and the fact that about 70% of the world's population occupies the coastal plain zones [5,6]. The intensity of

the problem depends on the amount of the abstraction, in relation to the natural groundwater recharge, as well as on the well field location and design, the geometry, and the hydrogeological parameters of the pumped aquifer.

In recent years, there is an increasing interest in evaluating the extent of seawater intrusion in response to overexploitation and sea level rise [7]. Seawater intrusion phenomena have been reported with different degree, in almost all coastal aquifers around the globe. In the United Sates, saltwater intrusion into coastal aquifers has been identified in the eastern Atlantic [8–14], and the southern [15] and western Pacific [16–19] coasts.

Reference [20] provides an overview of saltwater intrusion in the 17 coastal states of Mexico, which is one of the most important cases around the globe. Seawater intrusion induced by groundwater development is also known in South America [21] and Australia [22]. In Africa, several cases of seawater intrusion into coastal aquifers have been reported [23] with case studies in Morocco [24–26], Tunisia [27], Algeria [28] and Dar es Salaam [29,30]. In Europe, seawater intrusion has been documented within many of the coastal aquifers, particularly along the North Sea [31,32] and the Mediterranean Sea and its eastern part in the archipelagos in the Aegean Sea [33–35].

The arid and semi-arid areas are mostly chronically water-stressed. The problem of seawater intrusion is more severe in arid and semi-arid regions where the groundwater constitutes the main freshwater resource, which is mostly non-renewable. At present, developing countries of the Mediterranean Basin in North Africa and Middle East face environmental pressures induced by high population growth, rapid urbanization, and deficient water sector services reflecting on improper management of water resources [36,37]. The shortage of water in the Mediterranean region has been affected by the impact of climate change (increase of temperatures, variation of precipitations and high potential of evapotranspiration). Once again, the impacts have different effects in the Mediterranean region: the semi-arid and arid regions of the basin are exposed to desertification, increasing salinity of freshwater and exhaustion of water sources. Climatic change will also alter the marine environment, with an expected rise in sea level modifying several shores of the Mediterranean countries. To overcome the consequences of water scarcity and climate change, the aquifers and groundwater seem to be the solution. Many of the most important water projects in these regions focus on fossil water creating a sort of "pumping race" between the countries that share common aquifers, where overexploitation of groundwater in these regions is the major cause of seawater intrusion problems [34,35,38–46]. Therefore, the main challenges in coastal areas in the semi-arid region are water conservation, management and planning of the water resources. This is further complicated with several complexities of the geological formations. With the semi-arid conditions, complex geological settings and over-shooting stresses, the aquifer system becomes extremely fragile and sensitive [1]. Despite a good amount of research in this field, it is still needed to understand the behavior of such complex system precisely and apply the result in reasonably larger scales.

In the western Mediterranean, the situation of the groundwater in the Maghreb countries (Egypt, Libya, Tunisia, Algeria and Morocco) in North Africa has been marked by continuous decreases of water levels in coastal aquifers reaching alarming values. This decrease, caused by the synergistic effects of drought, flooding, changing land use, pollution from agriculture and industrialization, has intensified the problem of seawater intrusion [1]. The Korba coastal aquifer situated in Cap-Bon, Tunisia, has been experiencing seawater intrusion since 1970 and currently the salt load in this unconfined aquifer has peak concentrations of 5–10 g/L [27,47]. The Algerian coastal aquifers have also not escaped overexploitation with the Mitidja aquifer suffering from seawater intrusion [28], especially during the dry season. This aquifer system has a steady decline in water level in the order of 20–50 m per decade, which increases the rate of seawater intrusion on an annual basis [48]. The origin of water salinity on the Annaba coast (North East Algeria) is attributed to several factors such as the geological features of the region, the climate and the salt deposits. The salinity increases steadily when approaching the sea, and indicates the influence of marine water [49]. In Morocco, areas have been identified in which saltwater intrusion occurs (Temara-Rabat; Nador: [24]; Saidia: [25], however the

aquifer system also contains marine deposits which contribute to the degradation of the groundwater quality. The rates of water abstraction in these areas have increased in the last 50 years, resulting in the lowering of the water table and eventually allowing seawater to intrude from coastal areas [50].

In the Nile delta, seawater intrusion has been observed 60 km inland as a result of excessive pumping [51]. An extensive saltwater body has developed from upper Egypt to eastern Libya in the past 50 years. The freshwater/saline water interface passes through the Qattara depression crossing the Libyan-Egyptian border and finally turning to the Southwest reaching the Tazerbo area, southeast Libya [1]. The development of the Siwa oasis from the deep Nubian Sandstone Aquifer is close to the freshwater/saline water interface, and could cause the saline water to intrude into the freshwater aquifer (Internationally Shared Transboundary Aquifer Resources Management [52]. The problem is further compounded since on the Libyan side large amounts of water are abstracted for urban development, causing saltwater intrusion along the Libyan coast. This overabstraction in combination with the sluggish flow of the Nubian Sandstone Aquifer causes the saline water body to encroach even further inland with considerable increases in salinity due to seawater intrusion and upconing of deep saline water [46,53].

Progressive seawater intrusion in the coastal aquifers of Libya has been experienced since 1930s because of its ever-increasing water demand from underground water resources. Since the 1960s, the risk of seawater intrusion is continuously threatening large coastal parts of the Jifarah Plain that forms one of the economically most significant areas in Libya, where TDS peaks up to 10 g/L are recorded [54]. Numerous irrigated regions are located near the coast, principally in the northern part of Jifarah Plain including Tripoli region, where extensive irrigated areas have been established in the late 1970s and have evolved into advanced agricultural production zones; these activities are primarily dependent on groundwater extraction.

In Tripoli, the seawater intrusion has steadily increased from 1960 to 2007, a period during which potable water was available from the aquifer. Since 1999, a loss of 60% in well production in the upper aquifer has been observed [55].

Because of the accelerated development of the coastal zone of Tripoli in the last decades, it is necessary to evaluate the saline water intrusion phenomena of the coastal aquifer to open different choices for the rational exploitation of the groundwater resources in this semi-arid zone avoiding the degradation of groundwater quality.

2. Introduction to the Study Area

Libya's coastal area is one of the important cases in the arid and semi-arid regions, it is a south Mediterranean country and has a shoreline extent of about 1750 km. Groundwater is the main source for potable, industrial and irrigation water because of its semi-desert climate. Inevitably, groundwater extraction has been in excess of replenishment because of the rapid increase in agricultural and economic activities in the last 50 years. This has resulted in water level decline and deterioration in quality, including invasion of seawater along the coastal regions.

This situation has led to two significant problems linked to human activity: (1) salinization due to the formation of large piezometric drawdown cones, which have induced seawater intrusion by reversing the hydraulic gradients into aquifers; and (2) direct input of nitrate mainly from fertilizers and sewage. Agriculture is based on intensive irrigation and fertilization to improve the soils.

The Jifarah Plain in the northwest of the country, located between the Mediterranean coast and the Jabel Naffusah Mountain in the south, contains more than 60% of the country's population and produces 50% of the total agricultural outputs. Tripoli area is a typical example showing the problems of coastal zones under high anthropogenic pressure in dryland regions. Tripoli city forms an almost rectangular area (763 km^2) between the Mediterranean Sea and the cities of Swani and Bin Gashir in the south (Figure 1). This area extends for about 20 km along Tripoli coastal area and about 22 km inland. Topography is rising towards the south and east, a general trend in overall Jifarah Plain, which is bounded to the south and east by Jebal Nafusseh Mountains. The shortage of good quality water from

surface sources has made groundwater to be very important in the study area. The scarcity of water in Tripoli is becoming more pronounced due to the increase of the population coupled with improvement of the standard of living over the last few decades, where the area of the study accommodates dense population with more than 1.5 million of inhabitants mostly concentrated in the coast.

The principal aquifer used by the population in Tripoli is the Upper Miocene-Pliocene-Quaternary aquifer system, called "first aquifer" or "upper aquifer"; intercalated thin clayey sand and marl series are dividing the aquifer into a number of horizons, all are considered as one unconfined unit [56]. The Tripoli upper aquifer is affected by different sources of salinization, most serious is seawater intrusion [54]. The aim of this study was to discover what processes have been responsible for variations in the chemical composition of groundwater in the upper aquifer of Tripoli and to recognize the different sources of pollution, and their relation to the intense water withdrawal.

The climate in the study area is arid to semi-arid and typically Mediterranean, with irregular annual rainfall. The average annual rainfall and evapotranspiration rates are 350 mm/year and 1520 mm/year, respectively [54]. The estimation of groundwater exploitation (in the whole Jifarah Plain) from the main upper aquifer shows that the total amount of groundwater pumped in the Jifarah Plain for domestic, industrial and agricultural uses amounts to 1201.30 Mm^3/year [54]. For drinking water supply and domestic wells, the overall amount pumped is 6% of the total amount of groundwater extraction. The yield of irrigation wells was estimated to be 1123 Mm^3/year, which is equal to 93% of the total amount of groundwater extraction. The industrial sector pumps only 1% of the total groundwater exploitation in the plain. Since 1996, the Great Man-Made River Project is supplying the plain with an amount of 149 million m^3/year of water. This amount has been considered in the total abstraction estimation [54].

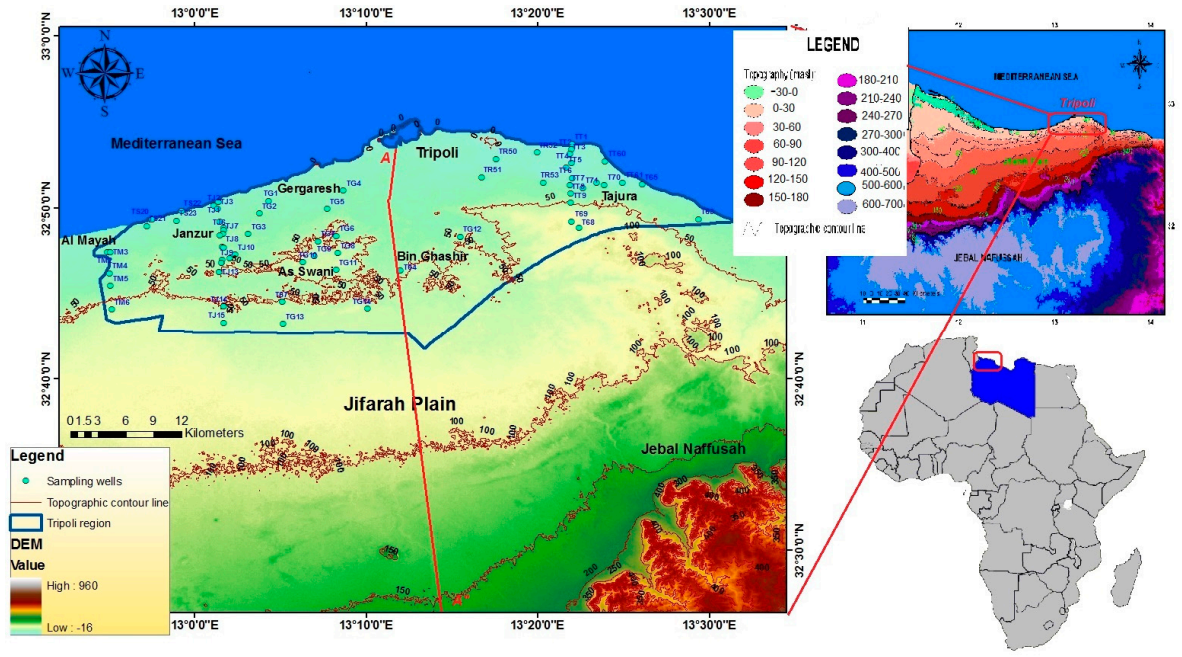

Figure 1. Location and topography of the study area in Jifarah Plain North West, Libya.

Geological and Hydrogeological Setting

The Jifarah Plain, including the study area, has been the subject of numerous geological studies [57–60].

Jifarah Plain is situated on the continental margin of Africa. Although the plain is thought to be underlain by Paleozoic rocks, the oldest encountered in boreholes are Triassic in age. These are continental, passing upwards into evaporites, a sequence thought to represent the progressive subsidence of the

margin during major Mesozoic extension of the Tethyan Ocean. Continued subsidence through the Jurassic and Early Cretaceous led to the deposition of marine sequences.

Figure 2 shows the geological cross-section in Jifarah Plain crossing Tripoli region. The location of the cross-section is indicated in Figure 1. The sediments of the Jifarah plain have been deposited since early Mesozoic times in a near shore lagoonal environment. The lithology of the upper aquifer varies widely and includes detrital limestone, dolomite, gravel, marl, clay, silt, sand, sandstone, gypsum/anhydrite and calcarenite. Middle Miocene clay separates the upper aquifer system in the area from the middle aquifer. The depth to the bottom of the upper aquifer varies between 30 and 200 m and depths of the wells that are utilizing this aquifer are between 10 and 180 m. Most of the wells tapping this aquifer give productivity of about 20–80 m^3/h [56].

The geological deposits, that are playing a role in the hydrogeology of the area comprising the Upper-Miocene-Pliocene-Quaternary formations, are given in Table 1.

The Pleistocene formations include terraces, which consist of cemented gravel and conglomerate. Al Kums Formation consists of limestone and dolomite. Qasr Al Haj Formation is mainly alluvial fans and cones consisting of clastic materials derived from the scarp. Jeffara Formation consists mainly of silt and sand, occasionally with gravel caliche bands; it covers extensive parts of the Jifarah Plain. Gergaresh Formation, which is known as Gergaresh Sandstone of Tyrrhennian age, occasionally contains silt lenses, conglomerate and sandy limestone.

The Holocene deposits include recent wadi deposits; these deposits consist of loose gravels and loam. Beach sands are represented by a narrow strip at the coast and are made up of shell fragments with a small ratio of silica sands. Eolian deposits are represented by sand dunes and sheets covering large parts of the coastal strip (coastal dunes). These coastal dunes consist of shell fragments with small amounts of silica sands. It is worth mentioning that the eolian material composing coastal dunes contains a large amount of grains of gypsum. In some places, it is composed of nearly pure gypsum (98%) especially in the immediate vicinity of the sebkhas, with a silty gypsum filling [58]. Sebkha sediments are mainly gypsum deposits and are observed along the coastal area of the plain. They occupy the relatively low topographic areas and are separated from the sea by sea cliffs. Some of the sebkhas have occasional incursions of the sea and others may have subsurface connection with the seawater.

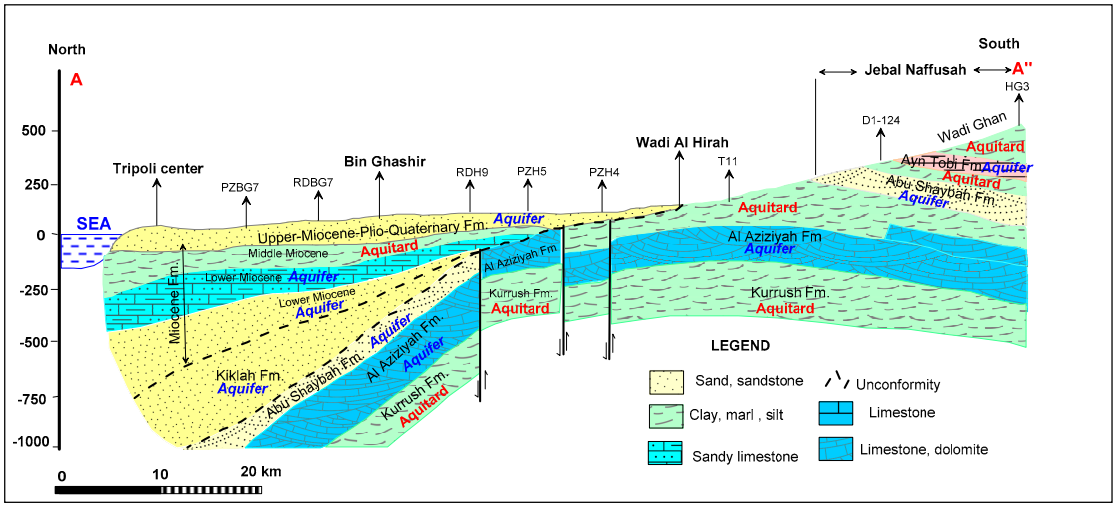

Figure 2. Geological cross-section in the coastal area of Jifarah Plain, including Tripoli region.

Table 1. Description of the Upper-Miocene-Pliocene-Quaternary deposits in the coastal area of Jifarah Plain around Tripoli.

Period	Epoch		Deposits and Formations	Typical Lithology	Thickness (m)
Quaternary	Holocene	Upper Miocene-Pliocene-Quaternary aquifer	Wadi deposits	Loose gravel, loam	5–150
			Sand beach	Shell and silica sand	
			Sand dunes and sand sheets	Shell fragments, silica sands and gypsum	
			Sebkha deposits	Gypsum	
			Fluvial-Eolian deposits	Silt, clay, marl and fine sand	
			Gergaresh Formation	Conglomerate, sandstone, silt, sandy limestone	
	Pleistocene		Jeffara Formation	Silt, sand and gravel caliche bands	
			Qsar al Haj Formation	Alluvial fans and cones	
			Al Kums Formation	Limestone, dolomite	
	Miocene		Volcanic rocks	Basalt and phonolite	25–250
		Middle	Middle Miocene clay		

3. Methodology

3.1. Sampling and Analytical Methods

A regional hydrogeochemical survey and water level measurements were performed during the dry period from September to November of 2008. A total of 64 shallow and deep wells (mostly 10–180 m deep), located at different distances from the Mediterranean Sea, were selected for groundwater sampling and water level measurement (see Figure 1). The samples were collected during pumping and the water level measurements were performed beforehand in static condition.

The sampling points were chosen along vertical lines perpendicular to the coast (Figure 1), with lengths comprised between 1 and 20 km, in order to explore the aquifer from inland to the coast line. Water depth was measured from the ground surface using water level meter, and was converted into water level by subtracting from ground elevation. The collected water samples were preserved in polyethylene bottles after filtering with 0.45 µm cellulose membrane filters. Two samples were taken from each well, one for determining anions, the other for determining cations. Samples for cation analysis were acidified to lower the pH to around pH = 2 by adding a few drops of nitric acid. Parameters measured are physical properties such as: pH, temperature, water level and electrical conductivity. Cations (Na^+, K^+, Mn^{2+}, Fe^{Total}, Ca^{2+}, Mg^{2+}, Zn^{2+}, and Si^{4+}) were analyzed using Flame Atomic Absorption Spectrometry (Varian). Anions (Cl^-, $NO_3{}^-$, $NO_2{}^-$, $SO_4{}^{2-}$, and $PO_4{}^{3-}$) and $NH_4{}^+$ were analyzed using the Molecular Absorption Spectrophotometer (Shimadzu). F^- was measured with ion selective electrode. Determination of carbonate ($CO_3{}^{2-}$) and bicarbonate ($HCO_3{}^-$) used the titration method with dilute HCl acid to pH 8.2 and 4.3, respectively. The above-mentioned analytical methods were used at the Laboratory of Applied Geology and Hydrogeology, Ghent University, and were provided in the Laboratory Manual and in Standard Methods for Examination of Water and Wastewater (American Public Health Association [61]. Careful quality controls were undertaken for all samples to obtain a reliable analytical dataset with an ionic balance error less than 5%.

3.2. Hydrochemical Evaluation Methods

The interpretation process is mainly based on the calculation of the ion deviations (Δm_i) from conservative freshwater/seawater mixing, the calculation of the saturation indices (SI), Stuyfzand classification system, graphical illustration methods including Piper diagram, calculation of ionic

ratios, and elaboration of hydrochemical profile and maps showing the spatial and vertical distribution of water quality parameters in the study area.

3.2.1. Saturation Indices

The PHREEQC 2.16 program [62] was used to calculate saturation indices for calcite, dolomite, halite and gypsum based on the chemical analytical results and measured field temperatures for all samples.

3.2.2. Ion Deviation from Conservative Freshwater/Seawater Mixing

Calculation of the ionic deltas Δm_i consists of a comparison of the actual concentration of each constituent with its theoretical concentration for a freshwater/seawater mix calculated from the Cl^- concentration of the sample [63], because Cl^- is the dominant ion in seawater and can be assumed to be conservative in many natural waters [64]. The ionic deltas quantify the extent of chemical reactions, affecting groundwater composition, next to mixing. The chemical reactions during fresh/seawater displacement can be deduced by calculating a composition based on the conservative mixing of seawater and freshwater, and comparing the conservative concentrations with those in the samples. The mass fraction of seawater (f_{sea}) in the groundwater can be obtained from chloride concentrations of seawater and freshwater as follows [64]:

$$fsea = \frac{m_{Cl^-,sample} - m_{Cl^-,fresh}}{m_{Cl^-,sea} - m_{Cl^-,fresh}} \quad (1)$$

where

$m_{Cl^-,sample}$ = the concentration of Cl^- in the sample expressed in mmol/L;

$m_{Cl^-,fresh}$ = the concentration of Cl^- in the freshwater expressed in mmol/L; and

$m_{Cl^-,sea}$ = Cl^- concentration in the seawater end member in mmol/L (for Mediterranean Seawater (possible end member), $m_{Cl^-,sea}$ = 645 mmol/L; Da'as and Walraevens, 2010).

Based on the conservative mixing of seawater and freshwater, the concentration of an ion i (m_i) in the mixed waters was calculated using the mass fraction of seawater f_{sea} as follows [64]:

$$m_i, mix = fsea \cdot m_i, sea + (1 - fsea) m_i, freshs \quad (2)$$

where m_i is concentration of an ion i in mmol/L and subscripts mix, sea, and fresh indicate the conservative mixture, and end members seawater and freshwater, respectively. Any change in concentration $m_{i,reaction}$ (Δm_i) as a result of reactions (not mixing) then becomes:

$$\Delta m_i = m_i, reaction = m_i, sample - m_i, mix \quad (3)$$

where $m_{i,sample}$ is the actually observed concentration in the sample in mmol/L.

The deviation from the conservative fresh/seawater mixing is due to chemical reactions. A positive delta means that the ion has been added to the water e.g., due to desorption from the exchange complex. Adsorption will lead to negative delta.

Ions in infiltrating rainfall near the coast are often derived from sea spray, and only Ca^{2+} and HCO_3^- are added due to calcite dissolution [64]. All other ions are thus ascribed to seawater admixture. In this case, $m_{i,fresh}$ = 0 for all components except Ca^{2+} and HCO_3^-.

The main end members used in the calculations for this study are the Mediterranean seawater and freshwater from the upper aquifer. For Mediterranean Seawater where Cl^- = 645 mmol/L, the seawater fraction has been calculated as:

$$fsea = \frac{m_{Cl^-,sample}}{645} \quad (4)$$

Table 2 shows the ion concentrations in rainwater, Mediterranean seawater end member and the freshwater end member in Tripoli (based on representative sample in Janzur TJ17).

Recharge water in the plain is the water flowing to the aquifer from the high topographic recharge area in the south (Jebal Naffusah). As no data were collected from the south border of the plain, the groundwater in the recharge area is expected to have the same composition as the freshwater samples collected from a nearby high topographic region, where the freshest water sample (i.e., sample TJ17) is considered as a reference sample to the composition of freshwater coming from the south. The recharge water in this sample has a high concentration of Ca^{2+} and HCO_3^- as a result of calcite dissolution. The analyzed recharge water in the plain is also showing considerable concentrations of Na^+, Mg^{2+} and SO_4^{2-} as a result of carbonate and evaporite dissolution in the unsaturated zone, and a great impact of concentration by evaporation, that is characteristic for the study area.

Table 2. Chemical composition of possible end members.

Parameter (Unit mg/L)	Analyzed Rainwater in Jifarah Plain	Analyzed Recharge Water in Tripoli (TJ17)	Mediterranean Seawater [54]
pH	7.64	7.97	-
Na^+	31.50	43.75	12,700
K^+	3.00	4.50	470
Ca^{2+}	13.40	49.51	470
Mg^{2+}	3.15	8.70	1490
Cl^-	26.10	55.15	22,900
SO_4^{2-}	10.33	36.62	3190
HCO_3^-	102.48	174.46	173
NO_3^-	1.12	29.10	0
NO_2^-	0.16	0.001	-
PO_4^{3-}	0.13	0.07	-
Fe (Total)	0.0	0.008	-
Mn^{2+}	0.01	0.01	-
NH_4^+	0.22	0.001	-
TDS	199.24	401.88	41,393

3.2.3. Stuyfzand Classification

The Stuyfzand classification [65–67] subdivides the most important chemical water characteristics at four levels: the main type, type, subtype, and class of a water sample (Tables 3–5). Each of the four levels of subdivision contributes to the total code (and name) of the water type.

The major type is determined based on the chloride content, according to Table 3. The type is determined based on an index for hardness (see Table 4), which can be expressed in French hardness degrees:

$$TH = 5 \times (Ca^{2+} + Mg^{2+}) \text{ in meq/L} \quad (5)$$

The classification into *subtypes* is determined based on the dominant cations and anions (Figure 3). First, the dominating hydrochemical family (and groups within families between brackets) is determined both for cations (Ca + Mg, (Na + K) + NH_4 or (Al + H) + (Fe + Mn)) and anions (Cl, HCO_3 + CO_3 or SO_4 + (NO_3 + NO_2)). The most important cation and anion (group: within a group: the dominant ion in that group) determine the name of the subtype. Finally, the *class* is determined based on the sum of Na^+, K^+ and Mg^{2+} in meq/L, corrected for a sea salt contribution (Equation (6)). This indicates if cation exchange has taken place and also the nature of the exchange, by assuming that all Cl^- originates from seawater, that fractionation of major constituents of the seawater upon spraying can be neglected and that Cl^- behaves conservatively.

$$\{Na^+ + K^+ + Mg^{2+}\} \text{ corrected} = [Na^+ + K^+ + Mg^{2+}] \text{ measured} - 1.061Cl^- \quad (6)$$

where

– = often pointing at a saltwater intrusion;
+ = often pointing at a freshwater encroachment; and
0 = often pointing at an equilibrium.

Each of the subdivisions contributes to the total code (and name) of the water type (see Table 5); for example, B4–NaCl– reads as: "brackish extremely hard sodium chloride water, with a $\{Na^+ + K^+ + Mg^{2+}\}$ deficit". This deficit is often due to cation exchange during saltwater intrusion (salinization). It is well known that the hydrogeochemical composition of coastal groundwater affected by seawater intrusion is mainly controlled by cation exchange reactions next to the simple mixing process [64]. These reactions can explain deviations of the concentrations of cations from conservative mixing of both waters.

Table 3. Water type classification [65].

Main Type	Code	Cl (mg/L)
Fresh	F	≤150
Fresh-brackish	Fb	150–300
Brackish	B	300–1000
Brackish-salt	Bs	1000–10,000
Salt	S	10,000–20,000
Hyperhaline	H	>20,000

Note: Division in main types based on chloride concentration.

Table 4. Subdivision of the main types based on hardness [65].

Number	Name	Code	Total Hardness (mmol/L)	Natural Occurrence in Main Types
−1	Very soft	*	0–0.5	F
0	Soft	0	0.5–1	F Fb B
1	Moderately hard	1	1–2	F Fb B Bs
2	Hard	2	2–4	F Fb B Bs
3	Very hard	3	4–8	F Fb B Bs
4	Extremely hard	4	8–16	Fb B Bs S
5	Extremely hard	5	16–32	Bs S H
6	Extremely hard	6	32–64	Bs S H
7	Extremely hard	7	64–128	S H
8	Extremely hard	8	128–256	H
9	Extremely hard	9	≥256	H

Note: * No code number.

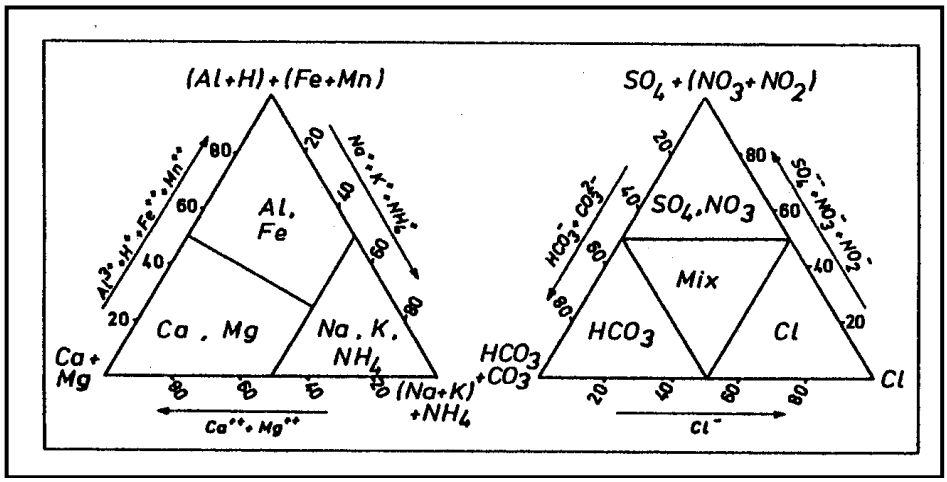

Figure 3. A ternary diagram showing the subdivision of types into subtypes [65].

Table 5. Subdivision of subtypes into classes according to $\{Na^+ + K^+ + Mg^{2+}\}$ corrected for sea salt [65].

Class	Code	Condition (meq/L)
{Na + K + Mg} deficit	-	{Na + K + Mg} corrected $< -\sqrt{0.5}$ Cl
{Na + K + Mg} equilibrium	0	$-\sqrt{0.5}$ Cl $\leq$ {Na + K + Mg} corrected $\leq +\sqrt{0.5}$ Cl
{Na + K + Mg} surplus	+	{Na + K + Mg} corrected $> \sqrt{0.5}$ Cl

4. Results and Discussion

4.1. Water Level and Hydrodynamics

Figure 4 shows a piezometric map of Tripoli based on field measurements. In the coastal area, 64 shallow and deep wells located at different distances from the Mediterranean Sea were selected for water level measurement (see Figure 1). Water depth was measured from the ground surface using water level meter and was converted into water level by subtracting from ground elevation.

The overall direction of groundwater flow in Jifarah Plain in general, is from the south from Jebal Naffusah Mountains to the coast. The important storage withdrawal by overexploitation from the upper aquifer in Tripoli is causing continuous drawdown of the water level, reducing the outflow rate to the sea, and the progressive degradation of the chemical quality of water. Groundwater level is mostly low, especially near the coast, where zero and negative heads are recorded for the majority of wells. The piezometric level in depression cones at the location of the public water supply well field of As Swani (123 wells) has dropped from 25 to 33 m below sea level (Figure 4), which testifies the inversion of the hydraulic gradient and the intrusion of seawater.

From Figure 4, it can be concluded that the general groundwater flow, from south to north following the topography, has altered, where, generally along the coast, flow is toward the reduced heads in the stressed areas around the depression cones.

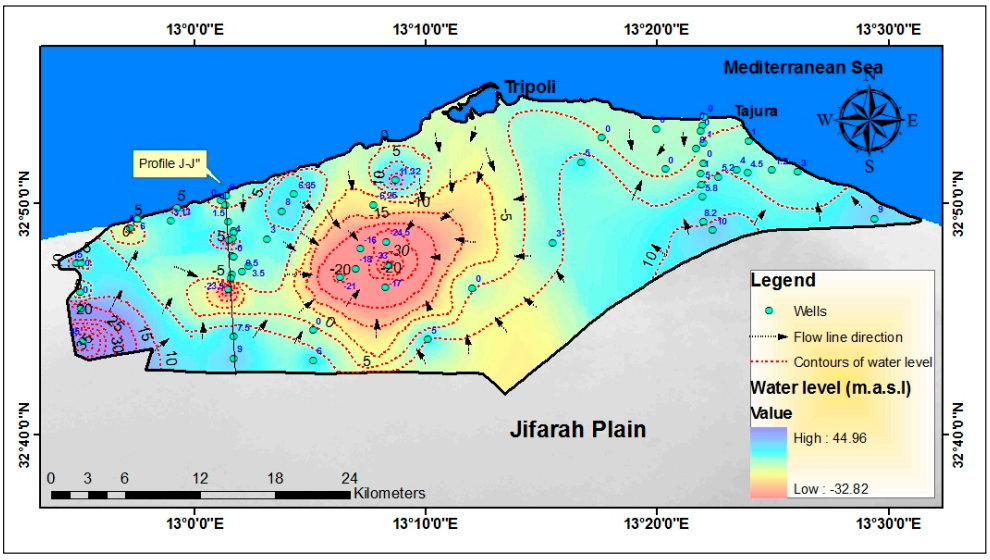

Figure 4. Tripoli piezometric map with flow vectors.

To deal with the shortage of water in most coastal cities including Tripoli region, the Libyan government established the Great Man-Made River Project (GMMR) to transport millions of cubic meters of water a day from desert well fields to the coastal cities, where over 80% of the population lives. Since 1996, The GMMR is supplying Tripoli city with an amount of 149 million m^3/year. The total planned supply by the project is 900 million m^3/year for the whole Jifarrah Plain. The implementation of the project was interrupted since 2011, due to political situation and Tripoli is the only supplied part of Jifarrah coast.

Since the start of the supply in 1996, the wellfield of As Swani (123 public water supply wells) was stopped. The pumping from As Swani wellfield is the main cause of the depression cone in Tripoli; the depression cone location at the center of As Swani wellfield is the most affected part of the region. Now the GMMR is the main supplier for domestic use in the city and being used also in many farms. The drawdown value around the depression cone is being reduced from 80 m below sea level in 1996 to 33 m in 2008.

4.2. Major Hydrochemical Parameters

Major anions and cations were analyzed and pH, Eh, electrical conductivity (EC) as well as temperature were assessed on all samples. The results show that: temperature ranges 18–25 °C, pH range is 7.17–9.94, Eh range is 139–240 mV, EC range is 369–10,600 µS/cm (25 °C), TDS range is 340–6529 mg/L and chloride concentration ranges 39–3155 mg/L. Table 6 shows analytical results for physico-chemical parameters of groundwater for selected representative samples in Tripoli. The high concentration of major ions such as Cl, Na, Ca, K, Mg, and a high EC indicate the presence of seawater in an aquifer [68,69].

Out of 64 samples analyzed, 38% have NO_3^- higher than the highest desirable level of 45 mg/L [70]. For sulfate 40% have SO_4^{2-} higher than the highest desirable level of 200 mg/L according to WHO (2008), with a maximum of 835 mg/L recorded southwards. Out of 64 analyzed samples, 58% exceed the recommended Cl^- value for standard drinking water (250 mg/L) and 26% have Cl^- greater than the highest admissible level of 600 mg/L [70].

Levels of Cl^- and EC are the simplest indicators of seawater intrusion or salinization [71,72]. EC is positively correlated with the concentration of ions, mainly Cl^- concentration. Figure 5 shows three zones on a plot of Cl^- vs. EC: freshwater zone, mixing zone and strong mixing (intrusion). It shows that groundwater samples with Cl^- exceeding 200 mg/L and EC exceeding ~1000 µS/cm are most likely influenced by seawater intrusion. Groundwater samples that are characterized by EC between 1000 and 5000 µS/cm represent a mixing between freshwater and saltwater. Samples with EC of more than 10,000 µS/cm represent strong seawater influence.

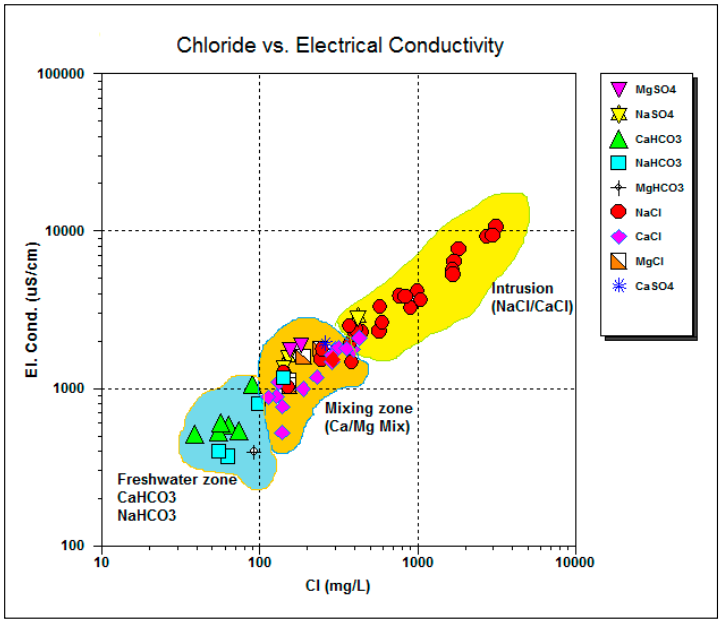

Figure 5. A plot of chloride vs. electrical conductivity showing fresh groundwater conditions, saltwater intrusion, and mixing between the two end members.

Table 6. Analytical results for physico-chemical parameters of selected groundwater samples in Tripoli.

ID	T (°C)	Water Level (m a.s.l)	pH	Eh (mV)	EC (µ/cm 25°)	Ca^{2+} mg/L	Mg^{2+} mg/L	Na^{+} mg/L	K^{+} mg/L	Mn^{2+} mg/L	$Fe^{2+/3+}$ mg/L	NH_4^{+} mg/L	NO_3^{-} mg/L	NO_2^{-} mg/L	CO_3^{2-} mg/L	HCO_3^{-} mg/L	Cl^{-} mg/L	SO_4^{2-} mg/L
TM5	22	19.11	7.30	234	2840	200	104	334	14	0.01	0.40	0.07	21	0.01	0	273	419	837
TM6	22	45.20	7.45	234	2500	110	72	283	6	0.01	0.41	0.19	118	0.01	0	219	371	382
TS21	21	−8.01	7.97	133	1160	82	42	99	8	0	0	0	11	0	6	287	142	91
TJ1	24	0	8.22	160	1826	172	29	186	16	0	0	0	16	0	24	269	316	221
TJ2	24	0	7.82	142	1940	93	84	160	6	0.01	0.01	0.02	69	0.11	0	323	376	123
TJ3	23	0	7.40	152	2380	140	93	184	14	0	0	0	83	0	0	317	410	268
TJ4	24	1.50	8.17	188	891	78	29	67	4	0	0	0	16	0	1	189	128	62
TJ5	24	2.25	8.16	143	1100	82	44	81	8	0	0	0	20	0	12	208	131	144
TJ6	22	1.50	7.59	161	524	71	40	76	5	0	0	0.03	73	0.11	0	236	138	87
TJ7	23	4.00	8.2	139	510	40	19	41	4	0	0	0	5	0	18	140	39	53
TJ8	23	3.80	8.19	156	878	62	36	67	4	0	0	0	18	0	12	165	113	96
TJ10	24	3.50	9.94	142	1020	66	41	79	5	0	0.08	0	53	0.14	0	198	151	115
TJ11	22	0	7.54	169	1530	116	65	90	6	0	0.12	0	79	0.10	0	220	290	148
TJ12	22	3.00	7.85	140	1592	72	64	111	6	0.01	0.04	0.10	46	0.11	0	190	189	161
TJ13	24	−23.90	7.77	150	1764	147	77	96	6	0.01	0.07	0.10	52	0.12	0	244	391	129
TJ14	24	7.50	8.20	198	1928	188	53	175	8	0	0	0	11	0	12	281	259	413
TJ15	24	9.00	7.30	175	1868	123	78	152	6	0	0.03	0.04	55	0.10	0	287	182	378
TJ17	23	23.00	7.97	213	532	50	9	44	5	0.01	0	0	29	0	0	175	55	37
TG1	19	26.35	7.75	149	2270	117	91	206	4	0.01	0.09	0.04	61	0.37	0	284	441	117
TG6	22	−24.50	7.40	151	7660	192	172	1023	22	0.01	0.16	0.04	77	0.12	0	232	1831	297
TR52	22	0	7.95	166	6380	132	137	1049	31	0	0	0	38	0	39	384	1709	274
TT2	22	0	7.73	148	9150	572	209	1129	70	0	0	0	0.80	0	6	421	2726	512
TT3	22	0	8.22	142	3850	262	100	377	67	0	0	0	1	0	24	433	766	418
TT6	21	0	7.73	162	9310	572	203	1178	20	0	0	0	23	0	3	226	3003	293
TT7	21	1.00	7.97	168	3810	204	108	480	24	0	0	0	6	0	12	256	840	567
TT9	24	5.80	8.30	183	600	50	24	48	8	0	0	0	7	0	9	189	57	67
T63	23	9.00	8.03	191	582	52	18	53	4	0	0	0	6	0	77	64	64	53

The spatial distribution of EC and Cl^- from analyzed groundwater samples across Tripoli city is presented in Figure 6a,b. In general, the EC, which is tightly linked to TDS, is a measure of salinity, and therefore is generally closely related to the Cl^- content. Both EC and Cl^- show the same general decrease from the Mediterranean shoreline towards the south. Frequent local increases in both variables are observed at the depression cones as a result of the high pumping rate.

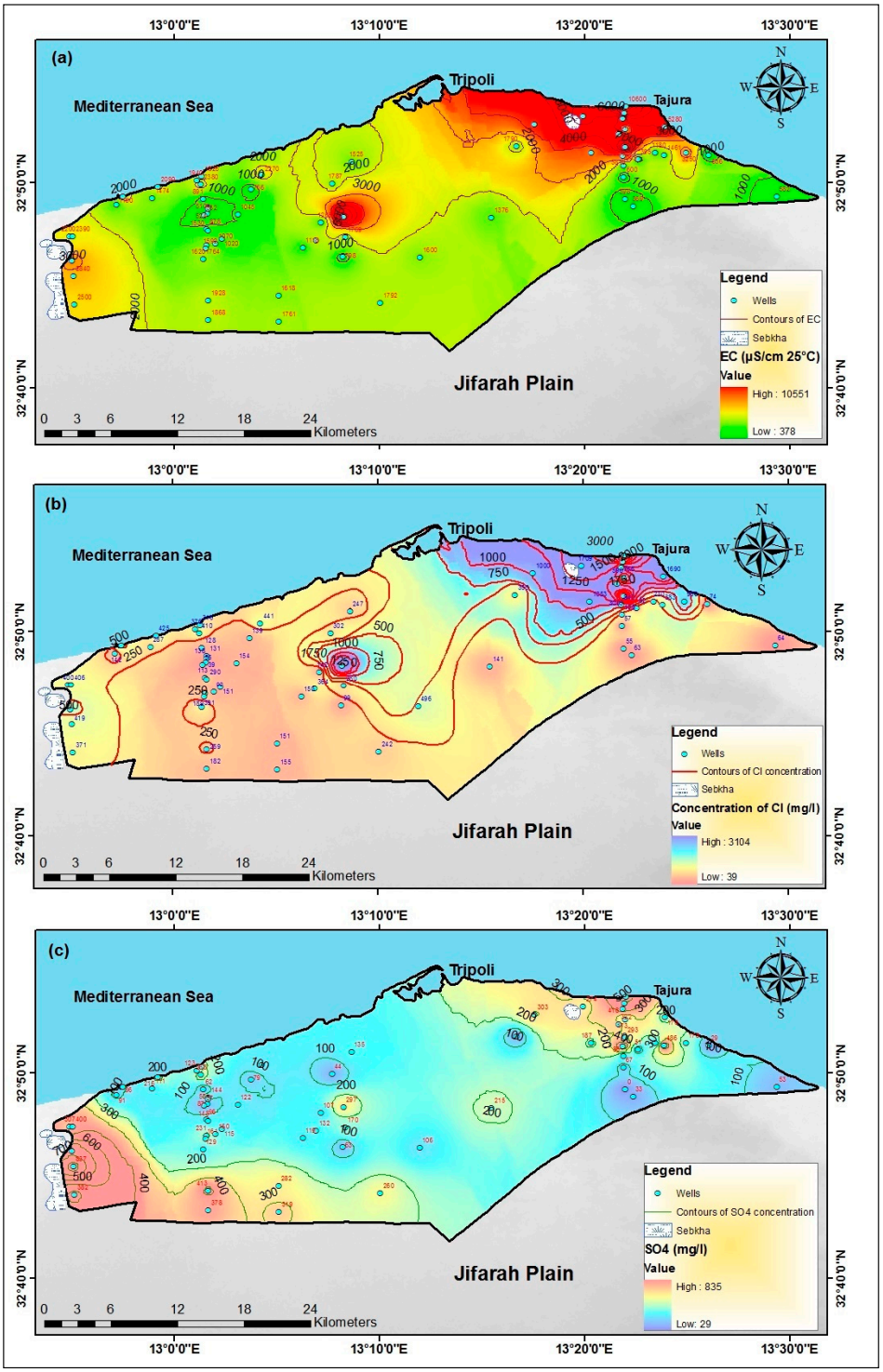

Figure 6. (**a**) Electrical conductivity map of Tripoli; (**b**) map with the spatial distribution of concentrations of Cl^-; and (**c**) spatial distribution of SO_4^{2-} in the upper aquifer of Tripoli.

The high Cl^- concentration is due to mixing with seawater. These high concentrations of chloride occur in most wells within a few kilometers of the coast, and are related to active seawater intrusion. However, high Cl^- is also found far inland at and nearby the depression cones, whereby deeper saline groundwater is affected by upconing due to groundwater exploitation. The concentration of Cl^- decreases gradually towards the south. However, in many farther inland wells, it is still the dominant anion. The higher concentration of Cl^- than the 250 mg/L value for standard drinking water at the south of the region can be linked to the synsedimentary marine influence of the groundwater.

Sulfate concentration in Tripoli ranges from 29 to 835 mg/L. Figure 6c shows the spatial distribution of SO_4^{2-} concentration in the study area. The main source for increasing SO_4^{2-} is mixing with seawater, which can add significant amounts of sulfate to freshwaters. High SO_4^{2-} is mostly linked to the high Cl^- concentration in the upper aquifer, both in the seawater intrusion zones and in the depression cones, where deep saline water upconing occurs.

Besides, more than 500 mg/L SO_4^{2-} is observed towards the west of region, with much higher SO_4^{2-}/Cl^- compared to seawater. The main source of SO_4^{2-} in this area is the dissolution of gypsum/anhydrite from the superficial sebkha deposits in those areas, as these wells are located near the vicinity of sebkhas. In this zone, lower Cl^- is recorded, excluding seawater intrusion as the source.

4.3. Water Types and Piper Diagram

Classification of hydrochemical facies for groundwaters according to the Piper diagram is represented in Figure 7.

In the Piper diagram, almost all water samples are plotted above the general seawater–freshwater mixing line [64], comprising freshwater sample TJ17 and Mediterranean Seawater. Although various hydrochemical facies were observed (NaCl, CaCl, MgCl, $CaMgHCO_3$, $NaHCO_3$, $NaSO_4$ $MgSO_4$ and $CaSO_4$), CaCl and NaCl types are dominant. Large proportion of the groundwater shows NaCl type, which generally indicates a strong seawater influence [50] or upconing of deep saltwater, while CaCl water type indicates salinization and cation exchange reaction [73]. The region of the CaCl type water may be a leading edge of the seawater plume [64,74,75]. Furthermore, sources of $CaSO_4$ water type are the dissolution of the scattered sebkha deposits.

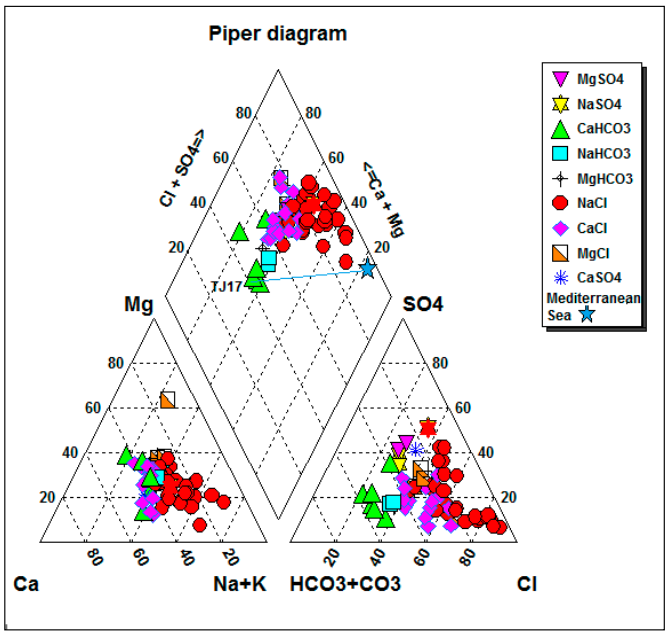

Figure 7. Water types according to Piper diagram.

4.4. Hydrochemical Profile and Water Classification According to Stuyfzand

Salinization is induced as the new saline end member is introduced into the freshwater aquifer. The main chemical reaction is cation exchange, resulting in deficit of Na^+ and surplus of Ca^{2+}:

$$Na^+ + 0.5Ca\text{-}X_2 \rightarrow Na\text{-}X + 0.5Ca^{2+}$$

where X represents the natural exchanger in the reaction. During cation exchange, the dominant Na^+ ions are adsorbed and Ca^{2+} ions released, so that the resulting water moves from NaCl to CaCl water type, which is typical for salinization [5]. The salinization process can be schematized as follows [75] (water types according to classification of Stuyfzand, [65]):

$$CaHCO_30 \Rightarrow CaCl^- \Rightarrow NaCl^- \Rightarrow NaCl0$$

$$F\ (fresh) \Rightarrow Fb\ (fresh\text{-}brackish) \Rightarrow B\ (brackish) \Rightarrow Bs\ (brackish\text{-}saline) \Rightarrow S\ (saline)$$

The chloride ion concentration is taken as a reference parameter [64]. Therefore, as saltwater intrudes into coastal freshwater aquifers, the Na/Cl ratio decreases and the Ca/Cl ratio increases.

Upon the inflow of freshwater, a reverse process takes place:

$$0.5Ca^{2+} + Na\text{-}X \rightarrow 0.5Ca\text{-}X_2 + Na^+$$

Flushing of the saline aquifer by freshwater will thus result in uptake of Ca^{2+} by the exchanger with concomitant release of Na^+. This is reflected in the increase of the Na/Cl ratio, and formation of the $NaHCO_3$ water type, which is typical for freshening. The anion $HCO_3{}^-$ is not affected because natural sediments behave as cation exchanger at the usual near-natural pH of groundwater [64]. The freshening process can be schematized as follows [73]:

$$NaCl0 \Rightarrow NaCl^+ \Rightarrow NaHCO^{3+} \Rightarrow MgHCO^{3+} \Rightarrow CaHCO^{3+} \Rightarrow CaHCO^30$$

$$S \Rightarrow Bs \Rightarrow B \Rightarrow Fb \Rightarrow F$$

The major hydrogeochemical processes occurring in the upper aquifer are: mixing with seawater end member, cation exchange during salinization, dissolution of gypsum from superficial sebkha sediments, carbonate dissolution and agricultural pollution.

The hydrogeochemical profile in Tripoli (Janzur) (Figure 8) is selected as an example showing the distribution of water types along the flow path. Janzur profile is about 14 km long perpendicular to the sea (see Figure 2). Seventeen wells were visited in this profile region. Their total depth is shallow (between 10 and 50 m) close to the coast, and reaches 120 m southward. They are pumping for irrigation in the private farms and for domestic use. The groundwater table in the profile is between 0 and 4 m a.s.l in the north, while it is down to −24 m a.s.l in the south at the depression cone. Groundwater is flowing from the south and north to the locally reduced heads, located at about 10 km from the coast.

The spatial distribution of water sub-types according to Stuyfzand in Tripoli is presented in Figure 9 together with the pie plot of TDS distribution for selected representative samples in Tripoli region. The water classification scheme of Stuyfzand [65] has the advantage that in brackish or saline groundwater, one can still identify many different water types even though the major anions and cations are the same and this may help to recognize processes such as upconing of more saline water in the aquifer [67]. Figures 8 and 9 show water type is $CaSO_4$ in the west, $CaHCO_3$, $NaHCO_3$, CaMix and MgMix towards the south and NaCl, MgCl and CaCl in the north and at the depression cones. Close to the shoreline and mainly in the east in Tajura the water is NaCl type, due to the strong effect of seawater intrusion. CaCl results from cation exchange, due to mixing with seawater. Towards the south, CaMgMix($ClHCO_3$) evolving further inland to CaMgMix(HCO_3Cl), indicates the location of the transition zone, where the groundwater changes from CaMgMix enriched with Cl^- ion to CaMix

with HCO_3^- as the dominant anion. The $CaSO_4$ water type observed in western Tripoli, up to about 14 km inland, shows the dissolution of the evaporitic rocks from the sebkha deposits.

The Mg^{2+} content found in several wells, is mainly resulting from the freshwater end member coming from the recharge area, where Mg^{2+}-containing carbonate is dissolved [54]. Thus, in this case, thee positive cation exchange code in the classification does not indicate freshening, as Mg^{2+} is not supplied by the marine end member [69]. At the depression cones and downstream, cation exchange equilibrium (cation exchange code "0") exists for several wells, which in this case indicates the onset of the salinization process (the positive value of $(Na^+ + K^+ + Mg^{2+})_{corrected}$ is decreasing as the marine cations are adsorbed during salinization).

The increase of salinity in Tripoli is accompanied by an increase in NO_3^- concentrations. Figure 8 also shows the spatial distribution of NO_3^- along Janzur profile. The average nitrate concentration of groundwater in the aquifer is about 38 mg/L, but contents as high as about 118 mg/L occur upstream in the south of the region. Irrigation with nitrogen fertilizers and domestic sewage and movement of contaminants in areas of high hydraulic gradients within the drawdown cones probably are responsible for localized peaks of the nitrate concentration for many wells in the region.

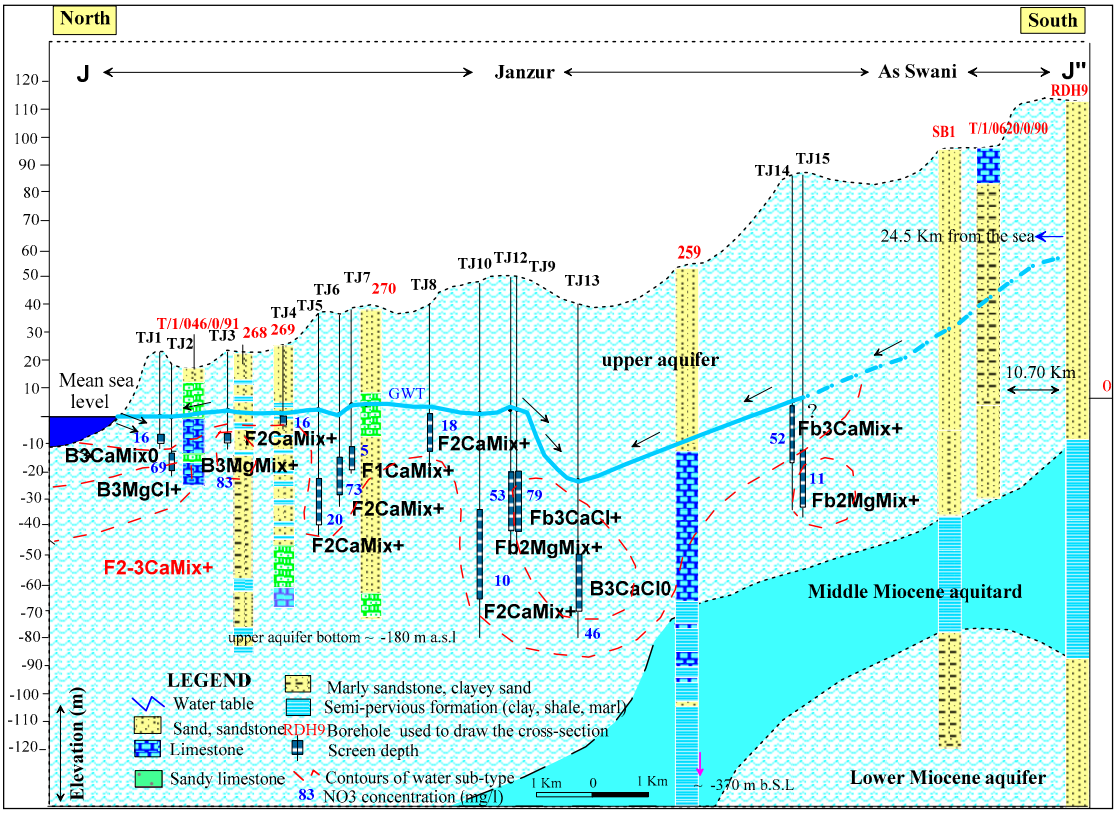

Figure 8. Hydrochemical profile in Tripoli (location of cross-section is indicated in Figure 2).

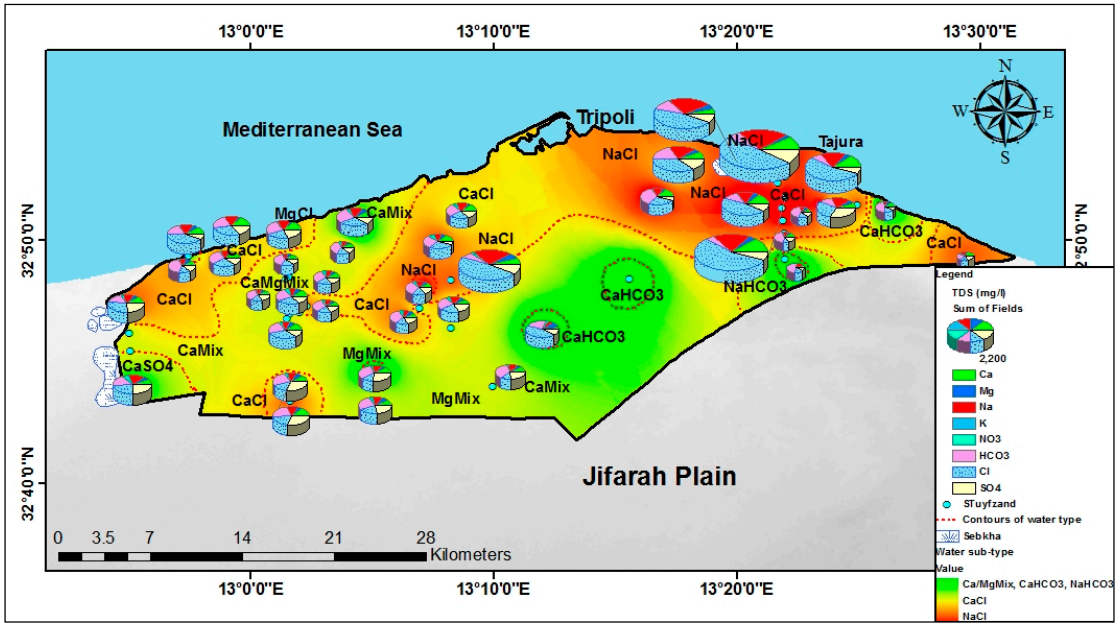

Figure 9. Distribution of water types according to Stuyfzand with a plot of TDS concentration for selected representative samples in Tripoli.

4.5. Ionic Ratio

Conservative seawater–freshwater mixing is expected to show a linear increase in Na^+ and Cl^- [76], which is reflected by the high correlation coefficient (r = 0.94) between both variables (Figure 10a). Effects of seawater encroachment have been evaluated by studying the Na/Cl ionic ratio. Lower ratios of Na/Cl than seawater values (0.88) indicate seawater encroachment. Figure 10b shows molar ratios of Cl^- versus Na/Cl concentrations. The Na/Cl ratios for the analyzed samples range from 0.23 to 1.68. Most of groundwater samples were less than or slightly higher than the Mediterranean seawater ratio (0.88). The lowered values with respect to the Mediterranean seawater ratio are resulting from cation exchange occurring when seawater intrudes freshwater aquifers, resulting in the deficit of Na^+ and surplus of Ca^{2+}. High ratio for several samples towards the recharge area (e.g., TJ17) indicates flushing the aquifer by freshwater from the south.

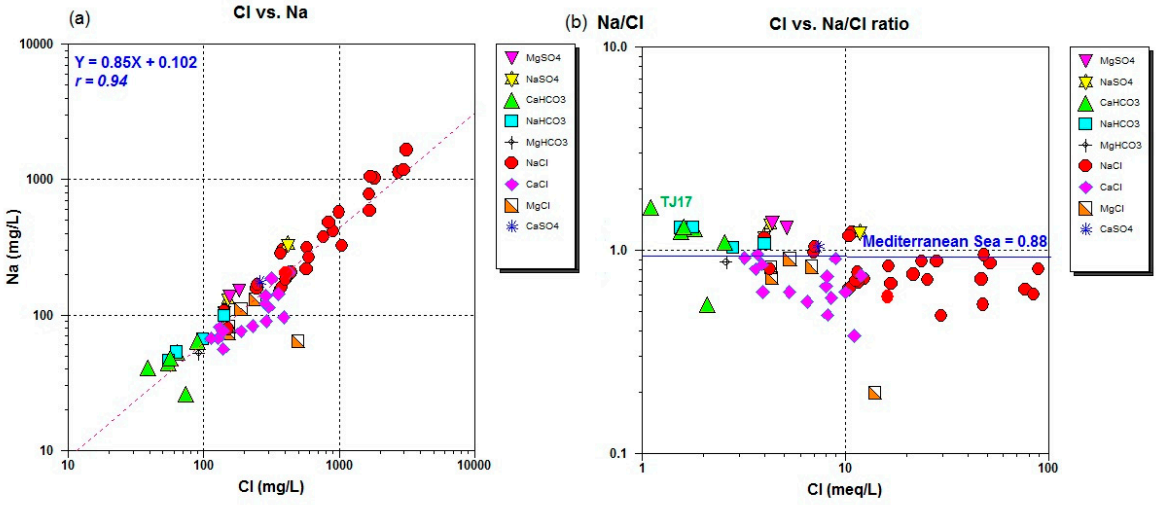

Figure 10. (**a**) Plot of Cl^- vs. Na^+; and (**b**) molar ratio of Cl^- vs. Na/Cl concentrations.

The ratio of SO_4/Cl (meq/L/meq/L) for the Mediterranean seawater and the fresh recharge water from the study area are 0.54 and 0.25, respectively. The ratio of SO_4/Cl for the analyzed samples ranges from 0.04 to 0.77, which indicates mixing between seawater and freshwater. Significantly higher values than Mediterranean seawater ratio (0.54) indicate dissolution of gypsum from Sebkha deposits.

The Na/K ratio is ranging in the area between 9.64 and 102.66, the largest values are observed in the area affected by the intrusion of seawater.

4.6. Saturation Indices

The saturation indices (SI) for calcite, dolomite, halite, aragonite, gypsum and anhydrite were calculated to verify precipitation and dissolution of these minerals. The selected minerals were based on the major ions in groundwater from the study area. Figure 11 is a synthetic diagram showing SI values for calcite, dolomite, gypsum, anhydrite, halite and aragonite. The sample numbers are sorted according to their location from west to east and from north to south with each profile, but they are not plotted at spatial distances.

Out of 64 groundwater samples, 80% of groundwaters seem to be supersaturated (SI > 0) with respect to calcite ($CaCO_3$), whereas 10% are undersaturated with respect to calcite (SI < 0) and 10% are at equilibrium (SI = 0). Dolomite ($MgCa(CO_3)_2$) seems to be oversaturated in 85% of groundwater samples analyzed, 5% are undersaturated and 10% are at equilibrium. Ninety-eight percent of groundwater samples in the study area are undersaturated with respect to gypsum ($CaSO_4 \cdot 2H_2O$) and anhydrite ($CaSO_4$).

In general, most of the analyzed samples have saturation indices close to saturation with respect to calcite (SI mostly 0–1) and dolomite (SI mostly 0–3). This slight supersaturation with respect to calcite and dolomite supersaturation rather points to groundwater in equilibrium with those minerals. During sampling, most often dissolved CO_2 gas escapes, slightly raising pH and thus shifting carbonate equilibrium (more CO_3^{2-}), such that SI > 0 is obtained, whereas in water in the aquifer SI with respect to calcite is close to zero. Thus, the water in the aquifer is not really oversaturated.

The majority of samples in the study area are undersaturated with respect to gypsum and anhydrite. Gypsum comes close to saturation (SI > −0.50) in several wells. The dissolution of gypsum from the superficial sebkha deposits for many wells in the coastal area raises the SI.

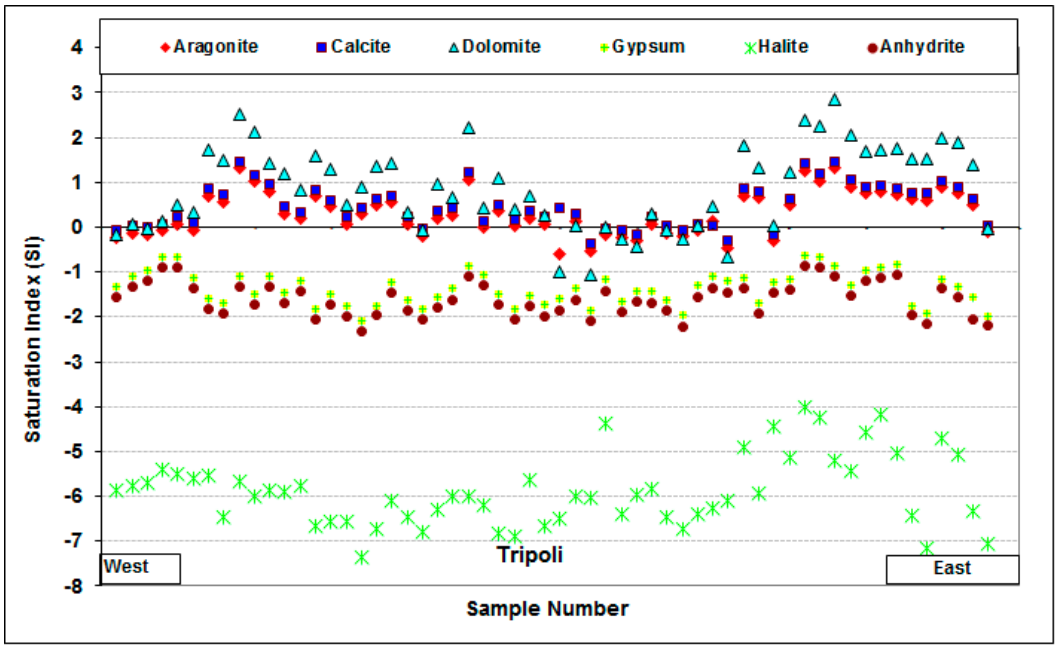

Figure 11. Calculated saturation indices of groundwater samples with respect to selected minerals.

4.7. Deviation from Conservative Mixture of End Member Fraction

Figure 12 shows the ionic deltas calculated for Na^+, Ca^{2+}, Mg^{2+}, K^+, HCO_3^- and SO_4^{2-} for all analyzed samples. The first thing to note is that the process of cation exchange due to salinization is very evident. For example, in Figure 12, $m_{Na^+,reaction}$ (ΔNa^+) is plotted in the secondary axis; the ΔNa^+ is usually positive for freshwater, but a large number of samples have negative values particularly in the highly saline water, down to −23 mmol/L. The most logical explanation for this deficit of Na^+ is that a reverse cation exchange reaction is taking place during the salinization process, which releases Ca^{2+} to the solution and captures Na^+. The reverse relationship between the two ions (Na^+ and Ca^{2+}) is noticed particularly in the highly saline groundwater, where samples with large negative values of ΔNa^+ generally show strong positive ΔCa^{2+}. Furthermore, also potassium shows negative (or very low positive) deltas characteristic for marine cations as a result of the salinization process.

ΔMg^{2+} is mostly positive, due to more Mg^{2+} added by dissolution of Mg^{2+}-rich carbonate than adsorbed at the clay exchange complex during salinization. Only very few samples show a deficit of Mg^{2+}. Figure 12 also shows that the ionic delta of ΔHCO_3^- is positive for most water samples. This is due to the dissolution of carbonate minerals in the aquifer deposits. In general, most samples show positive ΔSO_4^{2-}. The gypsum dissolution from sebkha deposits increases ΔSO_4^{2-} to high positive values for several wells.

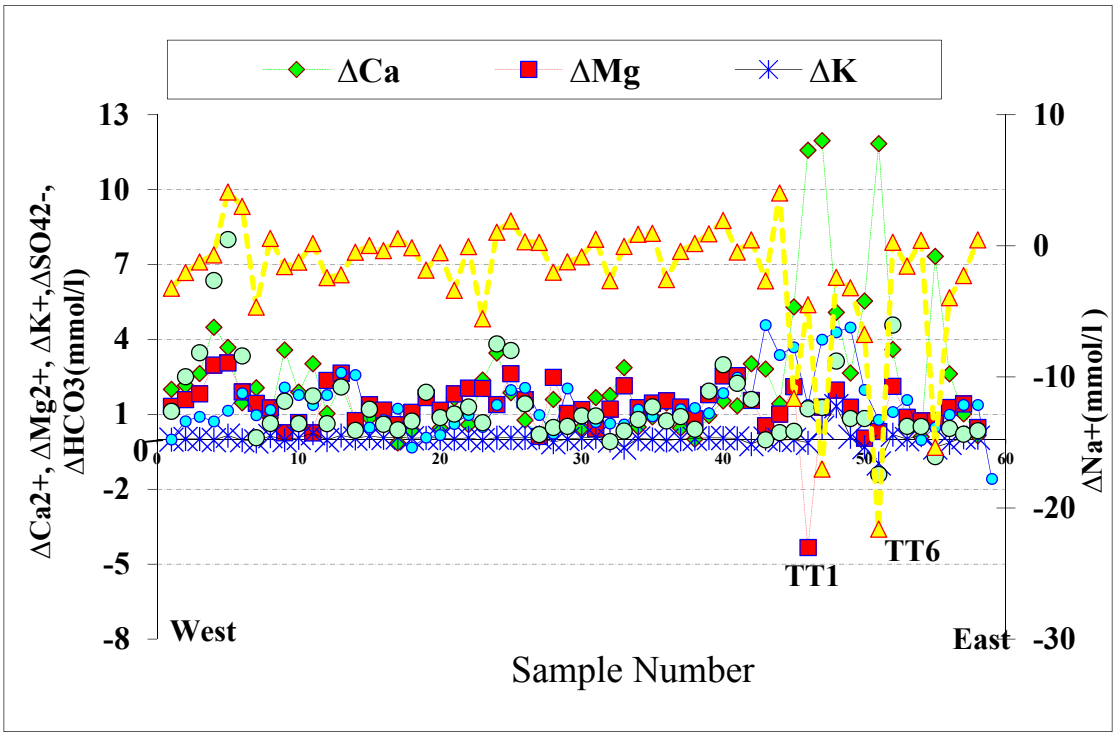

Figure 12. Diagram of ionic delta for all analyzed samples.

5. Conclusions

Hydrochemistry of the coastal aquifers of arid and semi-arid regions is very complex. Extensive groundwater extraction in Tripoli region, mainly for agricultural development, has caused substantial seawater encroachment and upconing of the deep saline water into Tripoli shallow aquifer, with Cl^-, SO_4^{2-} and NO_3^- as the major pollutants. In this study, this potential problem is investigated. The dominant water types in the study area are NaCl, CaCl and CaMgMix($ClHCO_3$) except for several wells towards the recharge area, where $CaHCO_3$-type prevails, and wells located near the superficial sebkha deposits, where the $CaSO_4$ water type evolves.

Seawater intrusion is accompanied by chemical reactions, which modify the hydrochemistry of the coastal aquifer. The most remarkable reaction is that of the inverse cation exchange, characteristic of the changes of the theoretical mixture of seawater–freshwater, which is carried out between clays and the aquifer water. This exchange consists in the release of Ca^{2+} and the adsorption of Na^{+}.

Great part of the observed high concentration of sulfate in Tripoli is coming from the effect of seawater intrusion. Furthermore, the scattered sebkha deposits in the north, containing large amounts of gypsum, produce high $SO_4{}^{2-}$ waters.

Another serious problem in the study area is the increased level of nitrate concentrations. It has been found that in large number of samples, nitrate contents range between 45 and 160 mg/L. The increased content originates from leaching of nitrates from the applied nitrogen fertilizers and from sewage. It is recommended that risk assessment of nitrate pollution is useful for a better management of groundwater resources, aiming at preventing soil salinization and minimizing nitrate pollution in groundwater.

The hydrochemical interpretation also indicates that the dissolution of calcite, dolomite and/or Mg^{2+} bearing calcite is an important process in most of the groundwaters. The saturation index shows mostly a slight tendency to precipitation of calcite and dolomite in the aquifer system, but this can be ascribed to lowering of CO_2 pressure at sampling, while in the aquifer, there is equilibrium with respect to these minerals.

Although the Great Man Made River Project is supplying Tripoli with an amount of 149 million m^3/year of water since 1996, used mainly for domestic purposes, results show high degradation level of groundwater quality and most of water samples do not compare favorably with WHO standards [70]; many samples exceed the maximum admissible concentrations, highlighting the degradation of groundwater quality. The recovery of groundwater quality is usually a very slow process as seawater intrusion is the result of a long-term negative mass balance in the aquifer. A balance between pumping demand and quality requirements is necessary. This balance is hard to maintain when the final goal is to reverse the qualitative status of the already contaminated aquifer. To protect the groundwater resource in the long-term, on which the future Tripoli residents depend, appropriate management against overexploitation from agricultural activity to control salinity is compelling, and especially urgent in the coastal fringe, where seawater intrusion is threatening. Artificial recharge of coastal aquifers, which are especially overexploited, may offer an efficient means of combating seawater intrusion and thus of preventing an inevitable degradation of the water quality which might prove irreversible.

Acknowledgments: This study was supported by the Libyan government through the Libyan Embassy in Brussels. Great thanks to the well owners and all who supported in the field campaigns.

Author Contributions: Alfarrah Nawal conceived and designed the research. Walraevens Kristine supervised the study.

Conflicts of Interest: The authors declare no conflict of interest.

References

1. Gaaloul, N.; Pliakas, F.; Kallioras, A.; Schuth, C.; Marinos, P. Simulation of Seawater Intrusion in Coastal Aquifers: Forty Five'Years exploitation in an Eastern Coast Aquifer in NE Tunisia. *Open Hydrol. J.* **2012**, *6*, 31–44. [CrossRef]
2. Masciopinto, C. Simulation of coastal groundwater remediation: The case of Nardò fractured aquifer in Southern Italy. *Environ. Model. Softw.* **2006**, *21*, 85–97. [CrossRef]
3. Mjemah, I.C.; Van Camp, M.; Walraevens, K. Groundwater exploitation and hydraulic parameter estimation for a Quaternary aquifer in Dar-es-Salaam, Tanzania. *J. Afr. Earth Sci.* **2009**, *55*, 134–146. [CrossRef]
4. Van Camp, M.; Mtoni, Y.E.; Mjemah, I.C.; Bakundukize, C.; Walraevens, K. Investigating seawater intrusion due to groundwater pumping with schematic model simulations: The example of the Dar Es Salaam coastal aquifer in Tanzania. *J. Afr. Earth Sci.* **2014**, *96*, 71–78. [CrossRef]

5. Jones, B.F.; Vengosh, A.; Rosenthal, E.; Yechieli, Y. Geochemical investigation of groundwater quality. In *Seawater Intrusion in Coastal Aquifers-Concepts, Methods and Practices*; Springer: Kluwer, The Netherlands, 1999; pp. 51–71.
6. Meybeck, M.; Vorosmarty, C.; Schultze, R.; Becker, A. Conclusions: Scaling Relative Responses of Terrestrial Aquatic Systems to Global Changes. In *Vegetation, Water, Humans and the Climate*; Kabat, P., Claussen, M., Dirmeyer, P.A., Gash, J.H.C., Bravo de Guenni, L., Meybeck, M., Pielke, R.A., Vorosmarty, C.J., Hutjes, R.W.A., Lutkemeier, S., Eds.; Springer: Berlin/Heidelberg, Germany, 2003; pp. 455–464.
7. Werner, A.D.; Bakker, M.; Post, V.E.A.; Vandenboede, A.; Lu, C.H.; Ataie-Ashtiani, B.; Simmons, C.T.; Barry, D.A. Seawater intrusion processes, investigation and management. Recent advances and futures challenges. *Adv. Water Resour.* **2013**, *51*, 3–26. [CrossRef]
8. Andreasen, D.C.; Fleck, W.B. Use of bromide: Chloride ratios to differentiate potential sources of chloride in a shallow, unconfined aquifer affected by brackish-water intrusion. *Hydrogeol. J.* **1997**, *5*, 17–26. [CrossRef]
9. Lin, J.; Snodsmith, J.B.; Zheng, C.; Wu, J. A modeling study of seawater intrusion in Alabama Gulf Coast, USA. *Environ. Geol.* **2009**, *57*, 119–130. [CrossRef]
10. Meisler, H.; Leahy, P.P.; Knobel, LL. *The Effect of Eustatic Sea-Level Changes on Saltwater-Freshwater Relations in the Northern Atlantic Coastal Plain*; U.S. Geological Survey Water-Supply Paper; U.S. Geological Survey: Reston, VA, USA, 1985; Volume 2255, p. 28.
11. Stringfield, V.T.; LeGrand, H.E. Relation of sea water to fresh water in carbonate rocks in coastal areas, with special reference to Florida, U.S.A. *J. Hydrol.* **1969**, *9*, 387–404. [CrossRef]
12. Wicks, C.M.; Herman, J.S. Regional hydrogeochemistry of a modern coastal mixing zone. *Water Resour. Res.* **1996**, *32*, 401–407. [CrossRef]
13. Wicks, C.M.; Herman, J.S.; Randazzo, A.F.; Jee, J.L. Water-rock interactions in a modern coastal mixing zone. *Geol. Soc. Am. Bull.* **1995**, *107*, 1023–1032. [CrossRef]
14. Barlow, M.P. *Groundwater in Freshwater-Saltwater Environments of the Atlantic Coast*; U.S. Geological Survey Circular: Reston, GA, USA, 2003; p. 1262.
15. Langman, J.B.; Ellis, A.S. A multi-isotope (δD, $\delta^{18}O$, $^{87}Sr/^{86}Sr$, and $\delta^{11}B$) approach for identifying saltwater intrusion and resolving groundwater evolution along the Western Caprock Escarpment of the Southern High Plains, New Mexico. *Appl. Geochem.* **2010**, *25*, 159–174. [CrossRef]
16. Izbicki, J.A. Chloride Sources in a California Coastal Aquifer, in Peters. In *Ground Water in the Pacific Rim Countries*; Peters, H.J., Ed.; American Society of Civil Engineers: Reston, GA, USA, 1991; pp. 71–77.
17. Izbicki, J.A. Use of δ ^{18}O and δD to define seawater intrusion. In *North American Water and Environmental Congress*; Bathala, C.T., Ed.; IR Div/ASCE; American Society of Civil Engineers: New York, NY, USA, 1996.
18. Todd, D.K. *Sources of Saline Intrusion in the 400-Foot Aquifer, Castroville Area, California*; Monterey Country Flood Control and Water Conservation District: Salinas, CA, USA, 1989; p. 41.
19. Vengosh, A.; Gill, J.; Davisson, M.L.; Hudson, G.B. A multi-isotope (B, Sr, O, H, and C) and age dating (^{3}H-^{3}He and ^{14}C) study of groundwater from Salinas Valley, California: Hydrochemistry, dynamics, and contamination processes. *Water Resour. Res.* **2002**, *38*. [CrossRef]
20. Cardoso, P. Raline water intrusion in Mexico. In *Water Pollution 2018*, 2nd ed.; Transactions on Ecology and the Environment; WIT Press: Southampton, UK, 1993. [CrossRef]
21. Bocanegra, E.; Da Silva, G.C.; Custodio, E.; Manzano, M.; Montenegro, S. State of knowledge of coastal aquifer management in South America. *Hydrogeol. J.* **2010**, *18*, 261–267. [CrossRef]
22. Werner, A.D. A review of seawater intrusion and its management in Australia. *Hydrogeol. J.* **2010**, *18*, 281–285. [CrossRef]
23. Steyl, G.; Dennis, I. Review of coastal-area aquifers in Africa. *Hydrogeol. J.* **2010**, *18*, 217–225. [CrossRef]
24. Chaouni Alia, A.; El Halimi, N.; Walraevens, K.; Beeuwsaert, E.; De Breuck, W. *Investigation de la Salinisation de la Plaine de Bou-Areg (Maroc Nord-Oriental)*; Freshwater Contamination; International Association of Hydrological Sciences—IAHS Publication: London, UK, 1997; Volume 243, pp. 211–220.
25. El Halimi, N.; Chaouni Alia, A.; Beeuwsaert, E.; Walraevens, K. Hydrogeological and Geophysical Investigation for Characterizing the Groundwater Reservoir in Saidia Plain (north-eastern Morocco). In *Development of Water Resource Management Tools for Problems of Seawater Intrusion and Contamination of Fresh-Water Resources in Coastal Aquifers*; Walraevens, K., Ed.; Ghent University: Ghent, Belgium, 2000; pp. 67–75, ISBN 90-76878-01-3.

26. Lamrini, A.; Beeuwsaert, E.; Walraevens, K. Contribution to the characterization of the Martil Coastal Aquifer System. In *Development of Water Resource Management Tools for Problems of Seawater Intrusion and Contamination of Fresh-Water Resources in Coastal Aquifers*; Walraevens, K., Ed.; Ghent University: Ghent, Belgium, 2000; pp. 76–81, ISBN 90-76878-01-3.
27. Tarhouni, J.; Jemai, S.; Walraevens, K.; Rekaya, M. Caractérisation de l'aquifère côtier de Korba au Cap Bon (Tunisie). In *Development of Water Resource Management Tools for Problems of Seawater Intrusion and Contamination of Fresh-Water Resources in Coastal Aquifers*; Walraevens, K., Ed.; Ghent University: Ghent, Belgium, 2000; pp. 11–27, ISBN 90-76878-01-3.
28. Imerzoukene, S.; Walraevens, K.; Feyen, J. Salinization of the coastal and eastern zones of the alluvial and unconfined aquifer of the Mitidja Plain (Algeria). In Proceedings of the 13th Salt Water Intrusion Meeting, Cagliari, Italy, 5–4 June 1994; pp. 163–175.
29. Van Camp, M.; Mjemah, I.C.; Alfarrah, N.; Walraevens, K. Modeling approaches and strategies for data-scarce aquifers: Example of the Dar es Salaam aquifer in Tanzania. *Hydrogeol. J.* **2013**, *21*, 341–356. [CrossRef]
30. Walraevens, K.; Mjemah, I.C.; Mtoni, Y.; Van Camp, M. Sources of salinity and urban pollution in the Quaternary sand aquifers of Dar es Salaam, Tanzania. *J. Afr. Earth Sci.* **2015**, *102*, 149–165. [CrossRef]
31. Oude Essink, G.H.P. Saltwater intrusion in 3D larg-scale aquifers a Duch case. *Phys. Chem. Earth* **2001**, *26*, 337–344. [CrossRef]
32. Vandenbohede, A.; Walraevens, K.; De Breuck, W. What does the interface on the fresh-saltwater distribution map of the Belgian coastal plain represent? *Geol. Belg.* **2015**, *18/1*, 31–36.
33. Alcala, F.J.; Custodio, E. Using the Cl/Br ratio as a tracer to identify the origin of salinity in aquifers in Spain and Portugal. *J. Hydrol.* **2008**, *359*, 189–207. [CrossRef]
34. Custodio, E. Coastal aquifers of Europe: An overview. *Hydrogeol. J.* **2010**, *18*, 269–280. [CrossRef]
35. De Montety, V.; Radakovitch, O.; Vallet-Coulomb, C.; Blavoux, B.; Hermitte, D.; Valles, V. Origin of groundwater salinity and hydrochemical processes in a confined coastal aquifer: Case of the Rhône delta (Southern France). *Appl. Geochem.* **2008**, *23*, 2337–2349. [CrossRef]
36. UN—United Nations. *Water for People, Water for Life*; UN World Development Report (WWDR); UN: New York, NY, USA, 2003.
37. WHO—World Health Organization. *Guidelines for Drinking-Water Quality: First Addendum to Third Edition, Volume 1 Recommendations*; WHO: Geneva, Switzerland, 2006.
38. Ben-Asher, J.; Beltrao, J.; Costa, M. Modelling the effect of sea water intrusion on ground water salinity in agricultural areas in Israel, Portugal, Spain and Turkey. In Proceedings of the International Symposium on Techniques to Control Salination for Horticultural Productivity, Antalya, Turkey, 7–10 November 2000.
39. Edmunds, W.M.; Milne, C.J. *Palaeowaters in Coastal Europe: Evolution of Groundwater Since the Late Pleistocene*; Geological Society of London: London, UK, 2001.
40. Gordu, F.; Motz, L.H.; Yurtal, R. Simulation of Seawater Intrusion in the Goksu Delta at Silifke, Turkey. In Proceedings of the First International Conference on Saltwater Intrusion and Coastal Aquifers Monitoring, Modeling, and Management, Essaouira, Morocco, 23–25 April 2001.
41. Yazicigil, H.; Ekmekci, M. Perspectives on Turkish ground water resources. *Ground Water* **2003**, *41*, 290–291. [CrossRef] [PubMed]
42. Karahanoglu, N.; Doyuran, V. Finite element simulation of seawater intrusion into a quarry-site coastal aquifer, Kocaeli-Darica, Turkey. *Environ. Geol.* **2003**, *44*, 456–466. [CrossRef]
43. Peters, H.J. *Ground Water in the Pacific Rim Countries*; IR Div/ASCE; American Society of Civil Engineers: New York, NY, USA, 1991; pp. 71–77.
44. Demirel, Z. The history and evaluation of saltwater intrusion into a coastal aquifer in Mersin, Turkey. *J. Environ. Manag.* **2004**, *70*, 275–282. [CrossRef] [PubMed]
45. Camur, M.Z.; Yazicigil, H. Effects of the planned Ephesus recreational canal on freshwater-seawater interface in the Selcuk sub-basin, Izmir. *Environ. Geol.* **2005**, *48*, 229–237. [CrossRef]
46. Alfarrah, N.; Hweesh, A.; Van Camp, M.; Walraevens, K. Groundwater flow and chemistry of the oases of Al Wahat, NE Libya. *Environ. Earth Sci.* **2016**, *75*, 1–24. [CrossRef]
47. Gaaloul, N.; Pliakas, F.; Kallioras, A.; Marinos, P. Seawater intrusion in Mediterranean porous coastal aquifers: Cases from Tunisia and Greece. In Proceedings of the 8th International Hydrogeological Congress of Greece, Athens, Greece, 8–10 October 2008; pp. 281–290.

48. World Bank. *People's Democratic Republic of Algeria—A Public Expenditure Review. Assuring High Quality Public Investment*; Report No. 36270; World Bank: Washington, DC, USA, 2007.
49. Djabri, L.; Laouar, R.; Hani, A.; Mania, J.; Mudry, J. The Origin of Water Salinity on the Annaba Coast (NE Algeria). In Proceedings of the Symposium HSO2a—IUGG2003, Sapporo, Japan, 30 June–11 July 2003; International Association of Hydrological Sciences—IAHS Publication: London, UK, 2003; Volume 280, pp. 229–235.
50. Pulido-Bosch, A.; Tahiri, A.; Vallejos, A. Hydrogeochemical characteristics of processes in the Temara Aquifer in Northwestern Morocco. *Water Air Soil Pollut.* **1999**, *114*, 323–337. [CrossRef]
51. Sherif, M.M. Nile Delta aquifer in Egypt. In *Seawater Intrusion in Coastal Aquifers—Concepts, Methods and Practices*; Bear, J., Cheng, A., Sorek, S., Ouazar, D., Herrera, A., Eds.; Theory and Application of Transport in Porous Media Book Series; Kluwer Academic Publishers: Dordrecht, The Netherlands, 1999; pp. 559–590.
52. ISARM. *Internationally Shared (Transboundary) Aquifer Resources Management*; IHP-VI, IHP Non Serial Publications in Hydrology November, Paris: UNESCO 2001; Internationally Shared (Transboundary) Aquifer Resources Management: Delft, The Netherlands, 2001.
53. Khouri, J. Water resources of the Zarka River basin, Jordan. In *Water Resources Management and Desertification Problems and Challenges*; World Meteorological Organization (WMO): Geneva, Switzerland, 1996; pp. 84–96.
54. Alfarrah, N. Hydrogeological and Hydrogeochemical Investigation of the Coastal Area of Jifarah Plain, NW Libya. Ph.D. Thesis, Laboratory of Applied Geology and Hydrogeology, Ghent University, Ghent, Belgium, 2011.
55. Alfarrah, N.; Berhane, G.; Bakundukize, C.; Walraevens, K. Degradation of groundwater quality in coastal aquifer of Sabratah area, NW Libya. *Environ. Earth Sci.* **2017**, *76*, 664. [CrossRef]
56. Alfarrah, N.; Van Camp, M.; Walraevens, K. Deducing transmissivity from specific capacity in the heterogeneous upper aquifer system of Jifarah Plain, NW-Libya. *J. Afr. Earth Sci.* **2013**, *85*, 12–21. [CrossRef]
57. Gefli. *Soil and Water Resources Survey for Hydro-Agricultural Development, Western Zone*; Unpublished Report; Ground Water Authority: Tripoli, Libya, 1972.
58. Libyan Industrial Research Centre (IRC). *Geological Map of Jifarah Plain*, 1st ed.; IRC: Tajura, Libya, 1975.
59. Kruseman, G.P. *Evaluation of Water Resources of the Gefara Plain*; Unpublished Report; SDWR: Tripoli, Libya, 1977.
60. Krummenacher, R. *Gefara Plain Water Management Plan Project*; Report on the Groundwater Resources of the Gefara Plain; Unpublished Report; 110p and 4 Annexes; GWA: Tripoli, Libya, 1982.
61. APHA (American Public Health Association). *Standard Methods for the Examination of Water and Wastewater*; Greenberg, A.E., Trussell, R.R., Clesceri, L.S., Eds.; APHA: Washington, DC, USA, 1985.
62. Parkhurst, D.L.; Appelo, C.A.J. *User's Guide to PHREEQC (Version 2)-A Computer Program for Speciation, Batch-Reaction, One-Dimensional Transport, and Inverse Geochemical Calculations*; U.S. Geological Survey Water-Resources Investigations Report 99-4259; U.S. Geological Survey: Reston, VA, USA, 1999; p. 312.
63. Fidelibus, M.D.; Tulipano, L. Regional flow of intruding seawater in the carbonate aquifers of Apulia (Southern Italy). In Proceedings of the 14th Salt Water Intrusion Meeting, Malmö, Sweden, 17–21 June 1996; Geological Survey of Sweden: Uppsala, Sweden, 1996.
64. Appelo, C.A.J. Cation and proton exchange, pH variations, and carbonate reactions in a freshening aquifer. *Water Resour. Res.* **1994**, *30*, 2793–2805. [CrossRef]
65. Stuyfzand, P.J. A new hydrogeochemical classification of water types: Principles and application to the coastal dunes aquifer system of the Netherlands. In Proceedings of the 9th SWIM, Delft, The Netherlands, 12–16 May 1986; pp. 641–656.
66. Stuyfzand, P.J. Hydrochemistry and Hydrology of the Coastal Dune Area of the Western Netherlands. Ph.D. Thesis, Free University (VU), Amsterdam, The Netherlands, 1993; p. 366.
67. Mollema, P.N.; Antonellini, M.; Dinelli, E.; Gabbianelli, G.; Greggio, N.; Stuyfzand, P.J. Hydrochemical and physical processes influencing salinization and freshening in Mediterranean low-lying coastal environments. *Appl. Geochem.* **2013**, *34*, 207–221. [CrossRef]
68. Mollema, P.N.; Antonellini, M.; Stuyfzand, P.J.; Juhasz-Holterman, M.H.A.; Van Diepenbeek, P.M.J.A. Metal accumulation in an artificially recharged gravel pit lake used for drinking water supply. *J. Geochem. Explor.* **2015**, *150*, 35–51. [CrossRef]

69. Mollema, P.N. Water and Chemical Budgets of Gravel Pit Lakes: Case Studies of Fluvial Gravel Pit Lakes along the Meuse River (The Netherlands) and Coastal Gravel Pit Lakes along the Adriatric Sea (Ravenna, Italy). Ph.D. Thesis, Technische Universiteit Delft, Delft, The Netherlands, 2016.
70. WHO—World Health Organization. *Guidelines for Drinking-Water Quality (Electronic Resource): Incorporating 1st and 2nd Addenda, Volume 1, Recommendations*, 3rd ed.; WHO Library Cataloguing-in Publication Data; WHO: Geneva, Switzerland, 2008; p. 668.
71. Mercado, A. The use of hydrogeochemical patterns in carbonate sand and sandstone aquifers to identify intrusion and flushing of saline waters. *Groundwater* **1985**, *23*, 635–664. [CrossRef]
72. El Moujabber, M.; Bou Samra, B.; Darwish, T.; Atallah, T. Comparison of different indicators for groundwater contamination by seawater intrusion on the Lebanese coast. *Water Resour. Manag.* **2006**, *20*, 161–180. [CrossRef]
73. Walraevens, K.; Van Camp, M. Advances in understanding natural groundwater quality controls in coastal aquifers. In Proceedings of the 18th Salt Water Intrusion Meeting (SWIM), Cartagena, Spain, 31 May–3 June 2004; pp. 451–460.
74. Vengosh, A.; Starinsky, A.; Melloul, A.; Fink, M.; Erlich, S. *Salinization of the Coastal Aquifer Water by Ca-Chloride Solutions at the Interface Zone, Along the Coastal Plain of Israel*; Hydrological Service: Jerusalem, Israel, 1991.
75. Jeen, S.W.; Kim, J.M.; KO, K.S.; Yum, B.W.; Chang, H.W. Hydrogeochemical characteristics of groundwater in a Midwestern coastal aquifer system, Korea. *Geosciences* **2001**, *5*, 339–348. [CrossRef]
76. Sanchez-Martos, F.; Pulido-Bosch, A.; Calaforra-Chordi, J.M. Hydrogeochemical processes in an arid region of Europe (Almeria, SE Spain). *Appl. Geochem.* **1999**, *14*, 735–745. [CrossRef]